

# Alternative Interpretation of Sharply Rising E0 Strengths in Transitional Regions

P. von Brentano<sup>1</sup>, V. Werner<sup>1</sup>, R.F. Casten<sup>1,2,3</sup>, C. Scholl<sup>1</sup>, E.A. McCutchan<sup>2</sup>, R. Krücken<sup>3</sup> and J.Jolie<sup>1</sup>

<sup>1</sup>*Institut für Kernphysik, Universität zu Köln, Köln, GERMANY*

<sup>2</sup>*Wright Nuclear Structure Laboratory, Yale University, New Haven Connecticut 06520-8124, USA*

<sup>3</sup>*Physik Department E12, Technische Universität München, 85748 Garching, GERMANY*

It is shown that strong  $0_2^+ \rightarrow 0_1^+$  E0 transitions provide a clear signature of phase transitional behavior in finite nuclei. Calculations using the IBA show that these transition strengths exhibit a dramatic and robust increase in spherical-deformed shape transition regions, that this rise matches well the existing data, that the predictions of these E0 transitions remain large in deformed nuclei, and that these properties are intrinsic to the way that collectivity and deformation develop through the phase transitional region in the model, arising from the specific  $d$ -boson coherence in the wave functions, and that they do not necessarily require the explicit mixing of normal and intruder configurations from different IBA spaces.

Phase transitions are a fundamental feature of many physical systems and have recently been of considerable interest, including extensive studies in atomic nuclei [1, 2, 3, 4, 5, 6, 7, 8, 9, 10, 11, 12, 13, 14, 15, 16, 17] and in other mesoscopic systems, *e.g.* [19]. One very active area of study has been the study of shape changes at low energy in nuclei [6, 7, 8, 9, 10, 11, 12, 13, 14, 15, 16, 17, 18] which have been described using catastrophe [6] and Landau theory [16, 17, 18]. Thus far, such studies have focused on data and model comparisons for energies, E2 transition matrix elements, and quadrupole moments. However, there has been little study of E0 matrix elements in these shape transitional regions despite the fact that, since such shape changes are inherently linked to changes in nuclear shapes and radii, the E0 operator and its transition matrix elements should provide a fundamental measure of how these phase transitions proceed [20].

To study this problem, we exploit the IBA model [21], which provides an economic and convenient approach to study both phase transitional behavior, in which a simple two term Hamiltonian of Ising type describes transitional regions in terms of variations of a single control parameter, and E0 transitions, for which the  $d$ -boson content is explicitly related to the deformation through the intrinsic state formalism [21, 22, 23].

There have, of course, been some studies of E0 transitions in transitional nuclei, most notably in the context of the IBA in the early work of Scholten *et al.* [24]. Their calculations for Sm isotopes provided anecdotal (*i.e.*, parameter-specific) evidence for an increase in E0 strength in deformed nuclei. Large values are also indicated in analytic expressions for  $\rho^2(\text{E0}; 0_2^+ \rightarrow 0_1^+)$  values in the O(6) and SU(3) limits [20, 21, 25, 26]. Estep *et al* [27] used calculations from ref. [28] in a shape coexistence formalism [29] to predict  $\rho^2(\text{E0}; 0_2^+ \rightarrow 0_1^+)$  values in the Mo isotopes (see below).

However, it is the purpose of this Letter to approach the question of E0 transitions in transitional nuclei in a much more general way, focusing on generic properties of  $\rho^2(\text{E0})$  values. We will use a simple but general Hamiltonian to span the full symmetry triangle [30] of the IBA and will display complete contours of these monopole

transitions that reveal robust, parameter-free characteristics of the model. As might be expected from our earlier comments, the most interesting behavior occurs precisely in shape transition regions, namely one finds a very sharp increase in  $\rho^2(\text{E0}; 0_2^+ \rightarrow 0_1^+)$ , which then *remains* large for well-deformed nuclei. We will show that, contrary to common opinion, this characteristic behavior of  $0_2^+ \rightarrow 0_1^+$  E0 transition strengths does *not* require an explicit mixing of coexisting spherical and deformed intruder configurations. Rather, it arises from a mixing of components with different  $d$ -boson content which is a natural ingredient in the IBA when U(5) symmetry is broken. By analyzing the calculated  $\rho(\text{E0})$  matrix elements in terms of contributions with different  $n_d$  values, we will show the key role of the  $d$ -boson coherence in the wave functions and that, while large  $n_d$  values are a necessary condition for large  $\rho^2$  values, they are definitely not a sufficient condition. Finally, while surprisingly little data exists on  $0_2^+ \rightarrow 0_1^+$  E0 transitions, much that does exist happens to be in shape transitional regions and we will see that the robust IBA predictions agree with these data.

We start with a simple IBM-1 Hamiltonian [14] that includes spherical-and deformation-driving terms whose competition determines the resulting structure,

$$H = a \left[ (1 - \zeta)n_d - \frac{\zeta}{4N_B} Q \cdot Q \right], \quad (1)$$

where  $Q = s^\dagger \tilde{d} + d^\dagger s + \chi (d^\dagger \tilde{d})^{(2)}$  with  $\chi \in [-\sqrt{7}/2, 0]$ . For  $\zeta = 0$  one obtains the U(5) limit while  $\zeta = 1$  and  $\chi = -\sqrt{7}/2$  gives SU(3), and  $\zeta = 1$  and  $\chi = 0$  gives O(6). In general, there is a spherical-deformed first order phase transition as a function of  $\zeta$  (except for  $\chi = 0$  where it is second order). The transition is most abrupt for  $\chi = -\sqrt{7}/2$  and occurs at  $\zeta = 0.5$  for large N, and at  $\zeta \sim 0.54$  for typical boson numbers ( $N \sim 10$ ). The E0 transition operator is [20, 24]

$$\rho(\text{E0}) = \alpha(s^\dagger s)^0 + \beta(d^\dagger \tilde{d})^0 = \alpha N + \beta'(d^\dagger \tilde{d})^0. \quad (2)$$

The first term vanishes for transitions and the connection to  $d$ -boson content is obvious. The results of our calculations, spanning the entire parameter space for  $N = 4, 10, \text{ and } 16$  are shown in Fig. 1A.

The essential result is immediately obvious, namely, that  $\rho^2(\text{E}0;0_2^+ \rightarrow 0_1^+)$  rises dramatically just in the shape transition region, and remains large in deformed nuclei. This qualitative result is independent of boson number (*i.e.*,  $N$ ,  $Z$ ), and of  $\chi$ . That is, there is no trajectory from spherical to deformed that avoids this increase. (Only the detailed trajectory of  $\rho^2$  depends on how  $\zeta$  and  $\chi$  vary.) This is a robust, parameter-free prediction of the model, inherent to its structure.

These large E0 transitions in the IBA raise a side issue that would be worth further exploration. The bosons in the IBA correspond to correlated pairs of nucleons in the valence space. Yet, microscopically, E0 transitions are forbidden in a single harmonic oscillator shell [20]. However, realistic shell model descriptions effectively entail mixing of several oscillator shells, which is reflected in the use of effective charges in calculations within restricted spaces. The IBA should incorporate such effects.

The sharp drop in  $\rho^2$  for  $\chi \rightarrow 0$  at lower right (going toward the O(6) limit) in the plots of Fig. 1A occurs because of a mixing and crossing of the  $0_2^+$  and  $0_3^+$  states. This is illustrated for  $N=10$  in Fig. 1B (left). Comparison with Fig. 1A shows that the  $0_2^+$  and  $0_3^+$  E0 strengths interchange, and large  $0_3^+ \rightarrow 0_1^+$  transitions emerge and persist into the O(6) limit where they are the allowed transition from the  $\sigma = (N-2) 0^+$  state [20]. If the  $0_3^+ \rightarrow 0_1^+$  and  $0_2^+ \rightarrow 0_1^+$  values are added, the contour plot remains nearly constant after the phase transition region [Fig. 1B (right)]. Other than this case, the only strong ground state E0 transition is  $0_2^+ \rightarrow 0_1^+$  although strong transitions between pairs of excited  $0^+$  states abound.

It is useful to decompose the E0 strengths in terms of individual components in the wave functions. This is done for  $N=10$  and  $\chi = -\sqrt{7}/2$  in Fig. 2 which shows, for three  $\zeta$  values (one before the transition, one near the critical point, and  $\zeta = 1$  for a well deformed rotor), the contributions to  $\rho(\text{E}0;0_2^+ \rightarrow 0_1^+)$  from each  $n_d$  value. These are calculated from  $\alpha_2(n_d)\alpha_1(n_d)n_d$  where  $\alpha_{1,2}(n_d)$  are the amplitudes in the  $0_1^+$  and  $0_2^+$  states with  $n_d$  bosons. In U(5), the  $0_1^+$  and  $0_2^+$  states have  $n_d = 0$  and  $n_d = 2$ , respectively and hence, by orthogonality,  $\rho(\text{E}0;0_2^+ \rightarrow 0_1^+) = 0$ . With increasing U(5) symmetry breaking by  $\zeta \rightarrow 1$ ,  $n_d$  is no longer a good quantum number. In fact, since  $\sum \langle 0_{i>1}^+ | n_d | 0_1^+ \rangle^2 = \langle n_d^2 \rangle - \langle n_d \rangle^2$ , the total E0 strength is related to the spreading (fluctuations) of  $n_d$  in the ground state. As higher  $n_d$  components grow [14, 21, 31] so do their contributions to  $\rho^2$ . Such  $d$ -boson mixing is inherently related to the onset of quadrupole deformation [21, 22, 23, 32].

Before the phase transition the  $\rho^2$  values are dominated by coherent  $n_d = 2, 3$  and 4 components. After the phase transition subtle positive and negative cancellations appear. Higher  $n_d$  components are essential to the final sum over  $\sum \alpha_1(n_d) \alpha_2(n_d) n_d$ . While finite  $d$ -boson amplitudes are clearly a necessary condition for both deformation and  $\rho$  values, large  $\rho$  values are not merely a trivial consequence of large  $\langle n_d \rangle$  values. The many small  $\rho(\text{E}0;0_i^+ \rightarrow 0_j^+)$  values prove this. This is

illustrated in the last panel of Fig. 2 which clearly shows the cancellations that give small  $\rho$  values for weak E0 transitions. Rather, it is the *specific d-boson coherence* in the wave functions that controls the resultant  $\rho$  values.

While the focus here is on  $0_i^+ \rightarrow 0_1^+$  transitions, we briefly comment on the behavior for higher spin. Calculations like those in Fig. 1, but for  $2_i^+ \rightarrow 2_1^+$  and  $4_i^+ \rightarrow 4_1^+$  E0 transitions, show similar behavior if the  $\rho^2$  strengths are summed over all initial states. However, there is more fragmentation. More than one initial state has E0 strength to the same yrast state for a given region of the triangle, and different initial states dominate the E0 decay in different regions. Empirically, ref. [20] lists a number of strong E0 transitions to the first  $2^+$  state and there seems to be enhanced fragmentation as well.

The robust predictions of  $\rho^2(\text{E}0;0_2^+ \rightarrow 0_1^+)$  demand experimental testing. E0  $0_2^+ \rightarrow 0_1^+$  transitions are known [20] in both the  $A = 100$  and 150 transition regions. Figure 3 compares these data with schematic IBA calculations, using  $\chi = -\sqrt{7}/2$  and  $N = 10$ . The data are plotted at  $\zeta$  values where the calculations reproduce the experimental  $R_{4/2}$  values. Despite the restriction to a fixed  $\chi$ , a constant boson number  $N$ , and that  $\zeta$  was chosen simply by fitting two yrast energies, these calculations clearly reproduce the sharp rise in  $\rho^2(\text{E}0)$  values.

These results raise an important question relating to phase transitional behavior. Microscopically, the Federman-Pittel mechanism [33], which invokes strong p-n interactions [34], leads to single particle energy shifts (via the monopole component [35]) and to the descent of a coexisting deformed configuration in otherwise spherical nuclei. An equilibrium deformation ensues when this configuration becomes the ground state. In the IBA, this coexistence can be explicitly included by the Duval-Barrett formalism [29] in which a pair of nucleons (protons in this case) is excited across a shell or subshell gap to form a space with  $N_{\pi def} = N_{\pi sph} + 2$  (counting the extra pairs of holes and particles as additional bosons), thus,  $H = H_{N_B} + H_{N_B+2} + H_{mix}$ . Typical Duval-Barrett calculations involve many parameters – two or more for each term in  $H$ . The calculations of ref. [28] used 13 parameters but reproduce the experimental  $\rho^2(\text{E}0;0_2^+ \rightarrow 0_1^+)$  values (see Fig. 3) in Mo rather well.

The interesting point, however, is that, while the large  $\rho^2$  values in these calculations have been ascribed [27] to the mixing, that is, to a non-vanishing  $H_{mix}$  (since, without  $H_{mix}$ , E0 transitions between states of  $H_{N_{\pi=1}}$  and  $H_{N_{\pi=3}}$  are forbidden), it is evident from Figs. 1 and 3 that large values of  $\rho^2(\text{E}0;0_2^+ \rightarrow 0_1^+)$  *also* occur in the IBA *without* the need to introduce such mixing.

How can these seemingly conflicting results be reconciled? Figure 5 of ref. [28] shows the probabilities of  $N_{\pi=1}$  and  $N_{\pi=3}$  components in the ground state wave functions (and, by orthogonality, the approximate admixtures for the  $0_2^+$  states). There is, in fact, little mixing (<10%) for  $N = 54$  (spherical Mo nuclei) and even less (<5%) for  $N = 60, 62$  (the first and second deformed Mo isotopes). *Only* for  $N = 56, 58$  is there substantial mix-

ing. Thus, these Duval-Barrett calculations effectively go over into the simple (single space) IBA results before and after the transition region. It is therefore *not* the large  $\rho^2$  value for  $N = 60$  that requires mixing. It is rather the *moderate*  $\rho^2$  values for the *pre-deformed* transitional Mo isotopes with  $N = 56, 58$ . This interpretation is validated by other observables. In  $^{96}\text{Mo}_{54}$ ,  $^{98}\text{Mo}_{56}$ , the experimental values of the ratios  $B(\text{E}2; 0_2^+ \rightarrow 2_1^+)/B(\text{E}2; 2_1^+ \rightarrow 0_1^+)$  and  $B(\text{E}2; 2_2^+ \rightarrow 2_1^+)/B(\text{E}2; 2_1^+ \rightarrow 0_1^+)$  *exceed* any predictions of standard models, including the vibrator and rotor. The reason is that the  $0_1^+$  state primarily consists of  $N$  bosons while the  $2_1^+$ ,  $0_2^+$  and  $2_2^+$  states belong primarily to the  $N + 2$  space [28]. Hence, the denominators are hindered. It requires the Duval-Barrett formalism with parameterized  $H_{mix}$  to account for these data.

The key point here is that large  $\rho^2(\text{E}0; 0_2^+ \rightarrow 0_1^+)$  values in transitional nuclei can arise in two ways, *either* from mixing of coexisting spherical and intruder configurations (as shown in ref. [26]) originating in different spaces (see ref. [36]), *or*, alternately, from the simpler IBA-1 itself. Thus, contrary to many statements in the literature, strong spherical-intruder state mixing is not *required* for large  $\rho^2(\text{E}0)$  values, *nor* are large experimental  $\rho^2(\text{E}0)$  values in transitional nuclei *necessarily* a signature of such mixing effects. One must analyze each region to determine whether to explicitly introduce shape mixing or whether the simple, few parameter, IBA alone suffices. In the Mo region ref. [28] shows that mixing of shape coexisting states is essential for the pre-deformed nuclei. However, in the first deformed nuclei in both the mass 100 ( $^{98}\text{Sr}$ ,  $^{100}\text{Zr}$ ,  $^{102}\text{Mo}$ ) and 150 ( $^{152}\text{Sm}$ ,  $^{154}\text{Gd}$ ) regions some of the largest known  $\rho^2(\text{E}0)$  values are easily accounted for *without* such mixing by the IBA-1.

We commented above that E0 transitions vanish in a single oscillator shell. It is therefore of interest to study how a valence space model such as the IBA, in which the bosons are considered to be formed from nucleons in the first open shell beyond an inert doubly magic core, can produce large E0 strengths. Of course, E0 transitions can arise by coupling to the giant monopole resonance, but this would seem to be outside the IBA space. Rather, the E0 transitions in the IBA may reflect the fact that realistic major shells in the independent particle model include an intruder orbit from the next higher shell, and that additional intruder orbits, from both lower and higher shells, appear in the Nilsson scheme with increasing deformation, that is, as the phase transition proceeds. Of course, as a phenomenological model, one cannot relate the IBA directly to such a picture without detailed microscopic analysis, but it may be that the importance of intruder orbits is reflected in the effective parameter,  $\beta'$ , in the E0 operator, which, in the calculations presented in Fig. 3, was fixed at  $6 \cdot 10^{-3}/eR_0^2$ . Remarkably, the

use of a simple one-body operator with constant coefficients is sufficient for reproducing the trends of the data in transition regions. Given the empirical success shown here for the simple IBA interpretation of E0 transitions, microscopic studies are strongly encouraged.

Lastly, one upshot of this study concerns well-deformed nuclei. The only  $\rho^2(\text{E}0; 0_2^+ \rightarrow 0_1^+)$  values known in the deformed rare earth nuclei are very small values ( $\rho^2 \sim 2 \cdot 10^{-3}$ ) in  $^{166}\text{Er}$  and  $^{172}\text{Yb}$ , in contrast to the IBA predictions. However, the empirical  $0_2^+$  states may not correspond to the  $0_2^+$  states of the IBA, but could have two-quasi-particle character. Interestingly, in the neighboring nucleus  $^{170}\text{Yb}$ , there is a rather strong E0 transition ( $\rho^2 = 27(5) \cdot 10^{-3}$ ) from the  $0_3^+$  state to the ground state. It is also interesting that there are a number of large  $\rho^2(\text{E}0; 2_i^+ \rightarrow 2_1^+)$  values known for deformed nuclei [20]. Moreover, in recent IBA calculations [37], anomalous kinks in the parameter systematics are avoided if the empirical  $0_3^+$  state is associated with the  $0_2^+$  IBA state near  $A = 170$ . Clearly, it is important to measure  $0_i^+ \rightarrow 0_1^+$  E0 transitions in a number of deformed nuclei to see if the total E0 strength predicted in the IBA is recovered.

To summarize, experimentally,  $\rho^2(\text{E}0; 0_2^+ \rightarrow 0_1^+)$  values rise dramatically in shape/phase spherical-deformed transition regions. We have presented here an alternative view in which this rise, and large E0 transitions in deformed nuclei, arise not from mixing of coexisting spherical and deformed configurations, although such a mechanism may contribute as well in specific instances (*e.g.*,  $^{98,100}\text{Mo}$ ), but rather from  $\beta$ -deformation and its variation in the transition region. This result is directly connected to the physics of phase transitional regions since calculations within a single space reproduce the characteristic increase in E0 transition strengths. That is, using the IBA-1 model, we showed that contrary to common opinion, the rise in  $\rho^2(\text{E}0)$  values is predicted even by this simple, single space model, that it agrees with the data, is parameter-free and intrinsic to the model, does not require the mixing of different IBA spaces, and develops due to the specific  $d$ -boson coherence in the wave functions. In the IBA-1 the E0 strengths are directly related to the fluctuations (spreading) in  $n_d$  values, and therefore to the  $\beta$ -deformation. Finally, we have proposed a direct test of these ideas through the measurement of E0 transitions to the ground state in well deformed nuclei.

We are grateful to T. Otsuka and F. Iachello for useful discussions, especially of the  $n_d$  content of the wave functions, and we thank B. Barrett for discussions on the Duval-Barrett formalism. Work supported by US-DOE grant number DE-FG02-91ER-40609, by DFG contract number Br 799/12-1, and by BMBF grant number 06K167.

---

[1] D. Warner, Nature (London) **420**, 614 (2002).

[2] A. Abbott, Nature (London) **403**, 581 (2000).

- [3] *Quark-Gluon Plasma 3*, edited by R.C. Hwa and X.-N. Wang (World Scientific, Singapore, 2004.)
- [4] J.B. Elliott *et al.*, Phys. Rev. Lett. **88**, 042701 (2002).
- [5] S. Liu and Y. Alhassid, Phys. Rev. Lett. **87**, 022501 (2001).
- [6] E. Lopez-Moreno and O. Castanos, Phys. Rev. C **54**, 2374 (1996).
- [7] R.F. Casten *et al.*, Phys. Rev. C **57**, R1553 (1998).
- [8] F. Iachello, Phys. Rev. Lett. **85**, 3580 (2000).
- [9] F. Iachello, Phys. Rev. Lett. **87**, 052502 (2001).
- [10] P. Cejnar and J. Jolie, Phys. Rev. E **61**, 6237 (2000).
- [11] J. Jolie, R.F. Casten, P. von Brentano, and V. Werner, Phys. Rev. Lett. **87**, 162501 (2001).
- [12] J.M. Arias, J. Dukelsky, and J.E. Garcia-Ramos, Phys. Rev. Lett. **91**, 162502 (2003).
- [13] J.M. Arias, Phys. Rev. C **63**, 034308 (2001)
- [14] V. Werner, P. von Brentano, R.F. Casten, and J. Jolie, Phys. Lett. B **527**, 55 (2002).
- [15] N.V. Zamfir, P. von Brentano, R.F. Casten, and J. Jolie, Phys. Rev. C **66**, 021304 (2002)
- [16] J. Jolie *et al.*, Phys. Rev. Lett. **89**, 182502 (2002).
- [17] P. Cejnar, S. Heinze, and J. Jolie, Phys. Rev. C **68**, 034326 (2003).
- [18] F. Iachello and N.V. Zamfir, Phys. Rev. Lett. **92**, 212501 (2004).
- [19] F. Iachello, F. Pérez-Bernal, and P.H. Vaccaro, Chem. Phys. Lett. **375**, 309 (2003).
- [20] J.L. Wood, E.F. Zganjar, C. De Coster, and K. Heyde, Nucl. Phys. **A651**, 323 (1999).
- [21] F. Iachello and A. Arima, *The Interacting Boson Model* (Cambridge University Press, Cambridge, 1987).
- [22] A.E.L. Dieperink and O. Scholten, Nucl. Phys. **A346**, 125 (1981).
- [23] J. Ginocchio and M. Kirson, Nucl. Phys. **A350**, 31 (1980).
- [24] O. Scholten, F. Iachello and A. Arima, Ann. Phys. (N.Y.), **115**, 235 (1978).
- [25] A. Arima and F. Iachello, Ann. Phys. **111**, 201 (1978).
- [26] K. Heyde and R.A. Meyer, Phys. Rev. C **37**, 2170 (1988).
- [27] R.J. Estep *et al.*, Phys. Rev. C **35**, 1485 (1987).
- [28] M. Sambataro and G. Molnar, Nucl. Phys. **A376**, 201 (1982).
- [29] P.D. Duval and B.R. Barret, Phys. Lett B **100**, 223 (1981).
- [30] R.F. Casten and D.D. Warner, in *Progress in Particle and Nuclear Physics*, vol. 9, ed. D. Wilkinson (Pergamon, Oxford, 1983), p. 311.
- [31] V. Werner, Diplomarbeit, Köln, 2000.
- [32] T. Otsuka, Hyperfine Interactions, **74**, 93. (1992).
- [33] P. Federman and S. Pittel, Phys. Lett. B **69**, 385 (1977).
- [34] I. Talmi, Rev. Mod. Phys. **34**, 704 (1962).
- [35] K. Heyde, P. Van Isacker, R.F. Casten, and J.L. Wood, Phys. Lett. B **155**, 303 (1985).
- [36] K. Heyde *et al.*, Phys. Rev. C **69**, 054304 (2004).
- [37] E.A. McCutchan *et al.*, to be published.

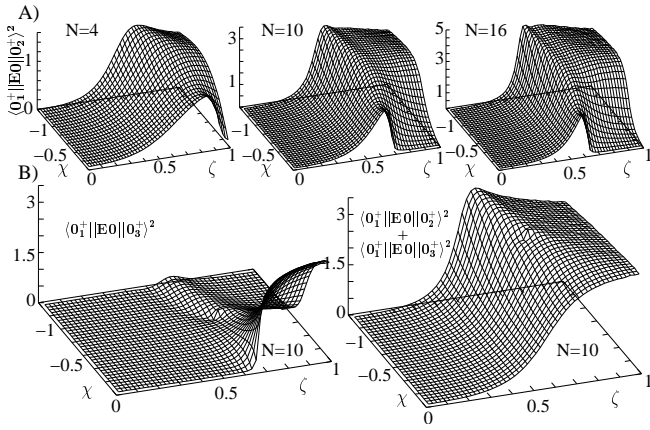


FIG. 1: A) Contour plots of  $\rho^2(E0;0_2^+ \rightarrow 0_1^+)$  throughout the IBA parameter space for  $N = 4, 10, 16$ . The range of  $\chi$  values implicit in the  $U(5)$  limit is explicitly shown along the left axis; B) Contour plots for  $N = 10$ , similar to the top panel, but for  $\rho^2(E0;0_3^+ \rightarrow 0_1^+)$  on the left and for the sum  $\rho^2(E0;0_2^+ \rightarrow 0_1^+) + \rho^2(E0;0_3^+ \rightarrow 0_1^+)$  on the right.

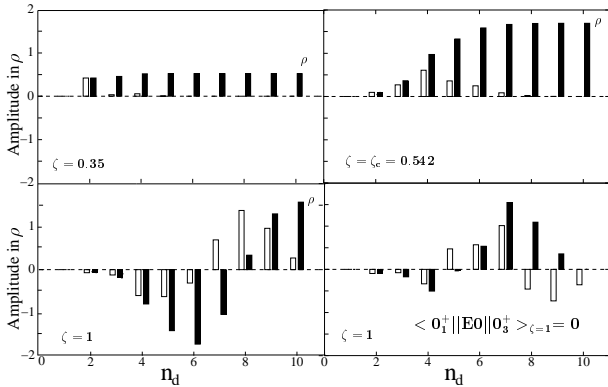


FIG. 2: Decomposition of the  $\rho(E0)$  amplitudes as a function of  $n_d$  for the  $0_2^+ \rightarrow 0_1^+$  transition for  $\zeta = 0.35, 0.54$  (near the critical point), and  $\zeta = 1$  and for  $0_3^+ \rightarrow 0_1^+$  for  $\zeta = 1$  at lower right, for  $N = 10, \chi = -\sqrt{7}/2$ . Open bars are amplitudes for a given  $n_d$  and solid bars are the running sum from  $n_d = 0$  up to the given  $n_d$  value.

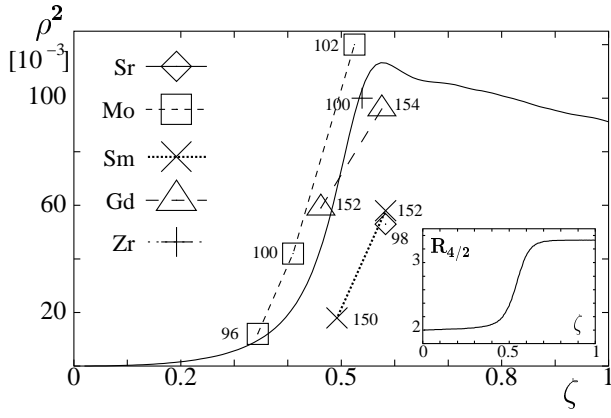


FIG. 3: Empirical  $\rho^2(E0;0_2^+ \rightarrow 0_1^+)$  values (from ref. [20]) for nuclei in the  $A = 100$  and  $150$  transition regions and schematic IBA-1 calculations. (As such schematic calculations cannot give  $R_{4/2} < 2$ , nuclei such as  $^{98}\text{Mo}$  are not considered.) The solid curve is the IBA prediction for  $N = 10$  with  $\chi = -\sqrt{7}/2$  and  $\beta'$  (eq. 2)  $= 6 \cdot 10^{-3}/eR_0^2$ . The inset shows how  $R_{4/2}$  itself behaves with  $\zeta$ : note the similarity to the  $\rho^2(E0)$  trajectory. Data points are labelled with mass number  $A$ .